SLOSHING OF LIQUIDS IN RIGID ANNULAR CYLINDRICAL AND TORUS TANKS DUE TO SEISMIC GROUND MOTIONS

M. Aslam,[I] W. G. Godden,[II] and D. T. Scalise[III]

SUMMARY

Sloshing response and impulsive hydrodynamic pressures in rigid axisymmetric tanks due to horizontal ground motions are predicted by theoretical solutions based on series and finite element analysis. Results are compared with experimental data from model tests conducted on a 20 ft × 20 ft earthquake simulator.

INTRODUCTION

The general problem of sloshing of liquid in containers due to dynamic excitation is one that has received considerable attention in the literature, and selected references are given [1,2,3,4]. This paper deals with sloshing in annular cylindrical and torus tanks due to horizontal seismic ground motions. Tanks of this type are used as pressure-suppression pools in Boiling Water Nuclear Reactors and have the following typical overall dimensions: annular tank - 120 ft. OD, 80 ft. ID, water depth - 20 ft.; torus tank - 140 ft. OD, 80 ft. ID, water depth - 15 ft.

Sloshing could lead to the danger of superheated steam escaping if, under dynamic conditions, the water level was to drop below Section C-C on the Mark III Suppression Pool of Fig. 1. Hence, it is important to be able to predict maximum water surface displacements for any prescribed seismic ground motion.

This paper presents the results of both experimental and analytical studies on the sloshing of water in both types of tanks subjected to arbitrary ground motions. Tests were done on model tanks on a shaking table. Two analytical procedures were developed; one based on a series solution and the other on the finite element method.

ANALYSIS

Assumptions: The analysis is based on three assumptions: (1) displacements are small and thus linear theory is applicable; (2) the tank is assumed to be rigid (the heavy structures used for suppression pools makes this a realistic assumption and even in more flexible tanks the assumption may still be valid as the primary sloshing response is a low frequency phenomenon); (3) water is assumed to be an incompressible and nonviscous fluid. Thus the flow remains irrotational.

I Senior Engineer, Bechtel Corporation, San Francisco, California.
II Professor of Civil Engineering, University of California, Berkeley, California.
III Department Head, Engineering Sciences Department, Lawrence Berkeley Laboratory, University of California, Berkeley.

The first solution (series solution) which involves Bessel functions is applicable to annular tanks. The second solution, based on the finite element method is applicable to all axisymmetric tanks. The velocity potential ϕ is taken as the primary variable and the sloshing displacements and impulsive pressures are derived from it. The equations of motion and both solutions are briefly described as follows:

Series Solution for Annular Tanks: In the annular tank of Fig. 2, as the flow is assumed to be irrotational there exists a velocity potential ϕ that must satisfy the Laplace equation,

$$\frac{\partial^2\phi}{\partial r^2} + \frac{1}{r}\frac{\partial\phi}{\partial r} + \frac{1}{r^2}\frac{\partial^2\phi}{\partial\theta^2} + \frac{\partial^2\phi}{\partial Z^2} = 0 \qquad (1)$$

Let a and b be the outer and inner radii of the annular tank and h be the depth of water, then the following boundary conditions must be satisfied:

$$\left.\frac{\partial\phi}{\partial r}\right|_{r=a} = \dot{x}\cos\theta \quad , \quad \left.\frac{\partial\phi}{\partial r}\right|_{r=b} = \dot{x}\cos\theta \quad , \quad \left.\frac{\partial\phi}{\partial z}\right|_{z=-h} = 0 \qquad (2\text{-}4)$$

in which $\dot{x} = dx/dt$ = tank wall velocity; and t = time. Also, the linearized free-surface boundary conditions is [5]

$$\frac{\partial^2\phi}{\partial t^2} + g\frac{\partial\phi}{\partial z} = 0 \quad \text{at} \quad z = 0 \qquad (5)$$

in which g = the acceleration of gravity. The solution to Eq. 1 subject to the above boundary conditions and at rest initial conditions is

$$\phi = \cos\theta\left[r\dot{x} - a\sum_{n=0}^{\infty} A_n \frac{\cosh\xi_n\left(\frac{z}{a}+\frac{h}{a}\right) C_1\left(\xi_n\frac{r}{a}\right)}{\omega_n\cosh\left(\xi_n\frac{h}{a}\right)} T_n(t)\right] \qquad (6)$$

in which

$$T_n(t) = \sin\omega_n t\int_0^t \dddot{x}\cos\omega_n\tau d\tau - \cos\omega_n t\int_0^t \dddot{x}\sin\omega_n\tau d\tau \qquad (7)$$

$$C_1\left(\xi_n\frac{r}{a}\right) = J_1\left(\xi_n\frac{r}{a}\right) Y_1'(\xi_n) - J_1'(\xi_n)Y_1\left(\xi_n\frac{r}{a}\right) \qquad (8)$$

$$A_n = \frac{2\left[\frac{2}{\pi\xi_n} - KC_1(K\xi_n)\right]}{\frac{4}{\pi^2}\xi_n^2(\xi_n^2-1) + C_1^2(K\xi_n)(1-K^2\xi_n^2)} \qquad (9)$$

and ξ_n are the roots of the equation

$$J_1'(\xi_n)Y_1'(K\xi_n) - J_1'(K\xi_n)Y_1'(\xi_n) = 0 \tag{10}$$

with $K = b/a$. The mode shapes are given by Eq. 8 and the frequencies ω_n are given by:

$$\omega_n = \frac{g}{a}\,\xi_n \tanh\left(\xi_n \frac{h}{a}\right) \quad , \tag{11}$$

In Eq. 8, J_1 and Y_1 are Bessel functions of the first and second kind and primes indicate their derivatives. Eq. 6 is the general expression for the velocity potential in an annular-circular tank. Once the expression for velocity potential is known, the surface displacements $\delta(r,\theta,o,t)$ and the impulsive hydrodynamic pressures $p(r,\theta,Z,t)$ anywhere in the fluid are derived from ϕ and given by the following expressions.

$$\delta(r,\theta,0,t) = -\frac{\cos\theta}{g}\left[r\ddot{x} - a\sum_{n=0}^{\infty} A_n \frac{\cosh\xi_n\left(\frac{z}{a}+\frac{h}{a}\right) C_1\left(\xi_n \frac{r}{a}\right)}{\cosh\left(\xi_n \frac{h}{a}\right)} \left(\cos\omega_n t \int_0^t \dddot{x} \cos\omega_n \tau d\tau + \sin\omega_n t \int_0^t \dddot{x} \sin\omega_n \tau \, d\tau\right)\right] \tag{12}$$

$$p(r,\theta,z,t) = -\rho\cos\theta\left[r\ddot{x} - a\sum_{n=0}^{\infty} A_n \frac{\cosh\xi_n\left(\frac{z}{a}+\frac{h}{a}\right) C_1\xi_n \frac{r}{a}}{\cosh\left(\xi_n \frac{h}{a}\right)} \left(\cos\omega_n t \int_0^t \dddot{x} \cos\omega_n \tau \, d\tau + \sin\omega_n t \int_0^t \dddot{x} \sin\omega_n \tau d\tau\right)\right] \tag{13}$$

Finite Element Analysis

Figure 4 shows a rigid wall tank of arbitrary shape filled with a liquid and whose free surface area is B2. B1 represents the surface area of liquid in contact with the solid boundary of the container. V is the volume of the liquid and δ is the surface water displacement. The velocity potential ϕ which must satisfy Laplace equation is written in rectangular coordinates as:

$$\frac{\partial^2\phi}{\partial x^2} + \frac{\partial^2\phi}{\partial y^2} + \frac{\partial^2\phi}{\partial z^2} = 0 \tag{14}$$

If $v_n(t)$ = velocity of the tank wall along its outward normal to the boundary at any point, then:

$$\frac{\partial\phi}{\partial n} = v_n(t) \quad \text{on B1} \tag{15}$$

For the finite element analysis we assume that

$$\phi = \sum_1^N N_j\,(x,y,z)\ \phi_j(t) \tag{16}$$

in which N_j *are the shape functions and* $\phi_j(t)$ are the nodal values of the field variable ϕ. Substituting Eq. 16 into Eqs. 14, 15 and 5, using the Galerkin principle [7,8,9,10,11] and applying the Divergence theorem we obtain:

$$\int_B N_i \left[\sum_1^N \frac{\partial N_j}{\partial x}\ell_x\phi_j + \sum_1^N \frac{\partial N_j}{\partial y}\ell_y\phi_j + \sum_1^N \frac{\partial N_j}{\partial z}\ell_z\phi_j\right] ds$$

$$-\int_v \left[\frac{\partial N_i}{\partial x}\sum_1^N \frac{\partial N_j}{\partial x}\phi_j + \frac{\partial N_i}{\partial y}\sum_1^N \frac{\partial N_j}{\partial y}\phi_j + \frac{\partial N_i}{\partial z}\sum_1^N \frac{\partial N_j}{\partial z}\phi_j\right] dv$$

$$= \int_{B1} N_i \sum_1^N \frac{\partial N_j}{\partial n}\phi_j ds - \int_{B1} N_i v_n ds$$

$$+ \frac{1}{g}\int_{B2} N_i \sum_1^N N_j \ddot{\phi} ds + \int_{B2} N_i \sum_1^N \frac{\partial N_j}{\partial z}\phi_j ds \tag{17}$$

in which $\ddot{\phi} = d^2\phi/dt^2$, $B = B1 + B2$, and ℓ_x, ℓ_y and ℓ_z are direction cosines, and $\int dv$ and $\int ds$ represent the integrals over the volume and appropriate surfaces respectively. Using the approximation $\partial N_i/\partial Z = \partial N_i/\partial n$, Eq. 17 can be simplified to the following form

$$\underline{M}\ddot{\phi} + \underline{K}\phi = \underline{F} \tag{18}$$

in which the elements of matrices $\underline{M}$, $\underline{K}$ and $\underline{F}$ are given by

$$M_{ij} = \frac{1}{g}\sum\int_{EB2} N_i N_j ds \tag{19}$$

$$K_{ij} = \sum\int_{EV}\left[\frac{\partial N_i}{\partial x}\frac{\partial N_j}{\partial x} + \frac{\partial N_i}{\partial y}\frac{\partial N_j}{\partial y} + \frac{\partial N_i}{\partial z}\frac{\partial N_j}{\partial z}\right] dv \tag{20}$$

$$F_i = \sum\int_{EB1} N_i v_n ds \tag{21}$$

where summation for M_{ij} covers only the elements on the free surface boundary and the integral is carried out on the free surfaces of each element EB2. Summation for K_{ij} covers the contribution of each fluid element and EV is the element region. EB1 refers only to the elements which lie on the solid boundary B1, and the loading term thus is associated with the elements that lie on the tank wall boundary. The free surface matrix $\underset{\sim}{M}$ and the fluid matrix $\underset{\sim}{K}$ are comparable to the mass and stiffness matrices respectively used in structural mechanics.

The finite element equations derived above apply to a general 3-dimensional case. However, in this study these equations were specialized to axisymmetric tanks [6] and the computer code was written to predict the hydrodynamic pressures p and sloshing displacements δ for arbitrary horizontal ground motions given by the following

$$\delta = -\frac{1}{g}\frac{\partial\phi}{\partial t} \tag{22}$$

$$p = -\frac{\rho\partial\phi}{\partial t} \tag{23}$$

in which ρ is the mass density of the fluid.

MODEL TESTS AND CORRELATION WITH ANALYSIS

Tests were conducted on a 20-ft × 20-ft (6-m × 6-m) shaking table at the University of California, Berkeley [12]. Annular tank tests used a 1/15th scale model of a Mark III suppression pool consisting of an 8 ft. (2.4-m) diameter steel tank with observation windows and an inside diameter of 5 ft. 6 in. (1.7 m) (Fig. 3). Torus tank tests used a 1/60th scale model of a Mark I suppression pool (Fig. 5). In both cases time-scaled accelerograms of the El Centro (1940) and Parkfield earthquakes were applied in increasing amplitudes to determine the range of linear behavior. Wave heights and dynamic pressures were recorded at selected locations.

Analytical results for wave heights as predicted by the series solution for annular tanks are compared with test data in Fig. 6 for two different intensities of the El Centro 1940 ground motion. In Fig. 6a the results are well within the linear range and comparison with theory is accurate, and this also applied to similar results for the ground motion applied at the actual intensity. Increasing the intensity by approximately 40% above actual produced some nonlinear behavior as shown in Fig. 6b. The range of linearity will depend on the predominant response mode as well as on the tank and the water depth: in the case shown the motion was primarily in the first radial mode and the limit of linearity was associated with a maximum water surface gradient of 1/5. The annular tank theory also gave good results for simple cylindrical tanks by letting the inner radius approach zero. Comparison of the finite element solution with the test results for the torus tank are shown in Fig. 7 and indicate a similar level of agreement. In both solutions the correlation between measured and computed hydrodynamic pressures was very close.

CONCLUSIONS

The correlation between measured and computed data indicate that the linearized small displacement theory developed for annular cylindrical or torus tanks can satisfactorily predict the sloshing displacements and hydrodynamic pressures in typical reactor suppression pools under the action of strong ground motions such as the El Centro 1940 and the Parkfield earthquakes. The theory is also applicable to plain cylindrical tanks by letting the inner radius approach zero.

REFERENCES

1. Bauer, H. F., "The Dynamic Behavior of Liquids in Moving Containers," National Aeronautics and Space Administration, Washington, D. C., 1966, edited by Abramson, H. Norman.

2. Clóugh, D. P., "Experimental Evaluation of Seismic Design Methods for Broad Cylindrical Tanks," Ph.D. Dissertation, University of California, Berkeley, 1976.

3. Veletsos, A. S. and Yang, J. Y., "Dynamics of Fixed-Base Liquid Storage Tank," U. S., Japan Seminar on Lifelines, 1976.

4. Luk, C. H., "Finite Element Analysis for Liquid Sloshing Problems," Office of Aerospace Research, U. S. Air Force Report No. 69-1504 TR, 1969.

5. Stoker, J. J., "Water Waves," Interscience Publishers, Inc., New York, N. Y. 1957.

6. Aslam, M., "Earthquake Induced Sloshing in Axisymmetric Tanks," Ph.D. Dissertation, University of California, Berkeley, 1978.

7. Crandall, S., "Engineering Analysis," McGraw-Hill, New York, 1965.

8. Finlaysan, B. A., "The Method of Weighted Residuals," Applied Mechanics Reviews, Vol. 19 No. 9, September 1966.

9. Hutton, S. G., "Finite Element Method-Galerkin Approach," Journal of Engineering Mechanics Division, Vol. 97 No. EM5, October 1971.

10. Zienkiewicz, O. C. and Perekh, C. J., "Transient Field Problems: Two-Dimensional and Three-Dimensional Analysis by Isoparametric Finite Elements," International Journal of Numerical Methods in Engineering, Vol. 2, No. 1, June 1970.

11. Pinder, G. P., "Application of Galerkin Procedure to Acquifer Problems," ASCE Journal of Water Resources, Vol. 8 No. 1, February 1972.

12. Rea, D., and Penzien, J., "Structural Research Using an Earthquake Simulator," Proceedings, Structural Engineering Association of California Conference, Monterey, California 1972.

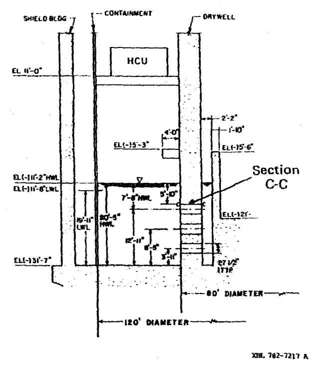

FIG. 1. Cross section through annulus of typical pressure suppression pool of boiling water reactor (Mark III).

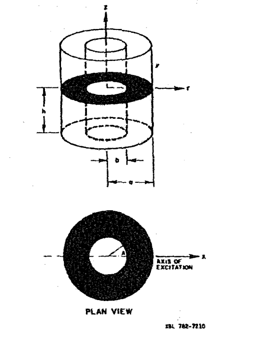

FIG. 2. Annular tank showing coordinate system.

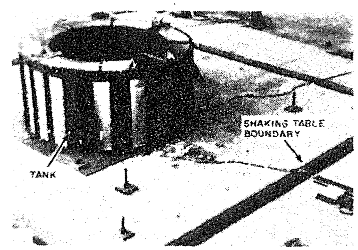

XBB 79-8772A

FIG. 3. 8-ft steel tank on 20 x 20 ft shaking table (1 ft = 0.305 m).

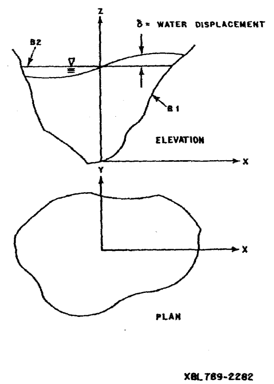

FIG. 4. Tank of arbitrary shape filled with liquid.

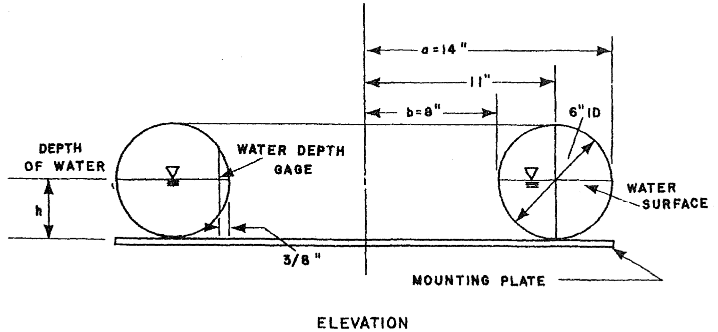

XBL 789-2279

FIG. 5. 1/60 scale model of Mark I pressure su

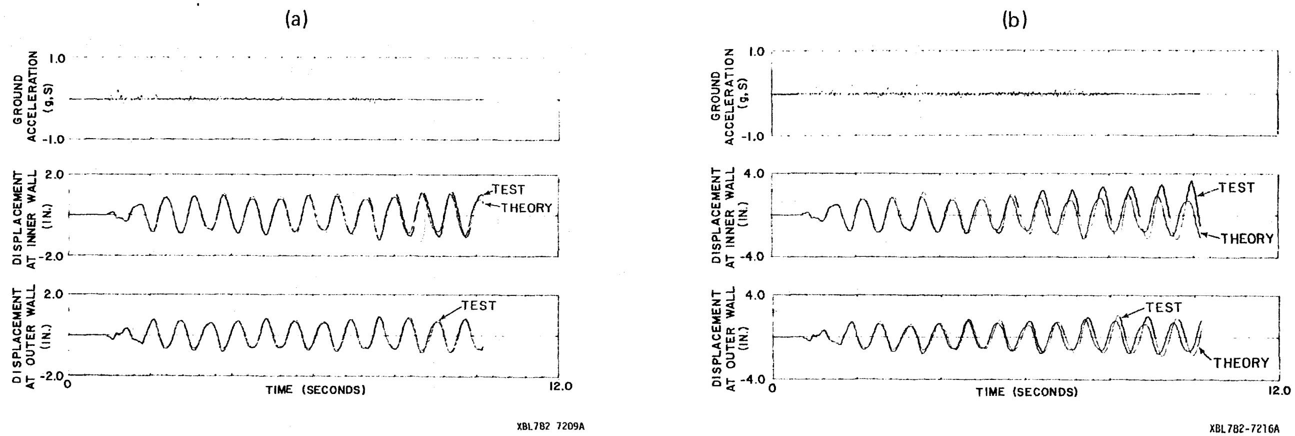

FIG. 6. Sloshing response of water in annular tank model (inner radius = 33.2 in., outer radius = 48.0 in., depth of water = 16.0 in.) under scaled El Centro 1940 earthquake. [Comparison of theory and test (1 inch = 25.4 mm)] (a) Peak acceleration = 0.24 g; (b) Peak acceleration = 0.44 g.

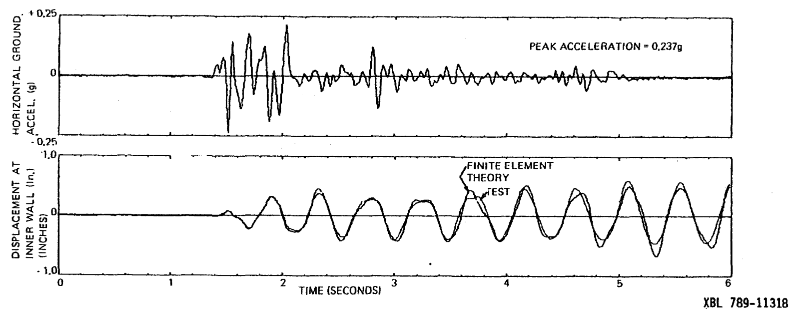

FIG. 7. Sloshing response of water in Torus Tank Model (inner radius = 8 in., outer radius = 14 in., depth of water = 3 in.). Test and finite element results for surface displacements.